Materials and Design 64 (2014) 714–720

Contents lists available at ScienceDirect

Materials and Design

journal homepage: www.elsevier.com/locate/matdes

Effects of tool rotational and welding speed on microstructure and mechanical properties of bobbin-tool friction-stir welded Mg AZ31

W.Y. Li [a,*,1], T. Fu [a], L. Hütsch [b], J. Hilgert [b], F.F. Wang [a], J.F. dos Santos [b], N. Huber [c]

[a] State Key Laboratory of Solidification Processing, Shaanxi Key Laboratory of Friction Welding Technologies, Northwestern Polytechnical University, Xi'an 710072, Shaanxi, PR China
[b] Helmholtz-Zentrum Geesthacht, Institute of Materials Research, Materials Mechanics, Solid-State Joining Processes (WMP), Geesthacht 21502, Germany
[c] Helmholtz-Zentrum Geesthacht, Institute of Materials Research, Materials Mechanics, Geesthacht 21502, Germany

ARTICLE INFO

Article history:
Received 12 June 2014
Accepted 11 July 2014
Available online 19 July 2014

Keywords:
Bobbin-tool friction stir welding
Magnesium alloy
Microstructure
Mechanical property

ABSTRACT

The effects of rotational and welding speeds on the microstructure and mechanical properties of bobbin-tool friction stir welded (BT-FSW) Mg AZ31 were investigated. The results indicated that the thermo-mechanically affected zone (TMAZ) consisted of equiaxed grains, which were inconsistent with the deformed, rotated and elongated grains found in the TMAZs of bobbin-tool friction stir welded Al alloys and friction stir welded Al and Mg alloys. The average grain size increased as the ratio of the rotational speed to welding speed increased. Excellent welds with no degradation in hardness were produced using a low heat input. Mechanical tests revealed that the ultimate tensile strengths gradually increased with increasing welding speed while keeping the rotational speed constant. The rotational and welding speeds had only slight influences on the yield stress and fracture elongation.

© 2014 Elsevier Ltd. All rights reserved.

1. Introduction

Recently, the increasing demand to reduce fuel consumption and associated costs has led to the replacement of heavy components with lighter alloys in the automotive and aerospace industries. Mg alloys have become a lucrative option for lightweight structures because of their low densities, high mechanical stiffnesses and environmental friendliness [1]. However, Mg alloys have a very strong affinity for oxygen and other chemical oxidants and can readily oxidize in the weld zone during fusion welding [2]. Other problems associated with conventional fusion welding of Mg alloys are related to defects that form during solidification, such as porosity, hot cracking, and partial melting, which degrade the mechanical properties of the joint. Therefore, a reliable joining technique is required to support the implementation of Mg alloys in the transportation industry.

Friction stir welding (FSW) is a solid-state joining technique, which was developed and invented by TWI Ltd. in 1991 [3]. This process avoids problems related to solidification when welding Mg alloys because of the avoidance of bulk melting during welding. Residual stresses and associated distortion can be notably reduced because the welding temperatures are significantly lower compared to those in conventional fusion welding techniques [2]. To date, FSW has been widely applied to join various Mg alloys, such as Mg–Al–Zn [4], Mg–Zn–Y [5] and Mg–Al–Ca alloys [6].

To enable welding of closed sections without the need of a backing bar, which is required in conventional FSW to accommodate the loads applied during welding, an alternative tool configuration has been proposed [3] named bobbin-tool friction stir welding (BT-FSW), as shown in Fig. 1. This process configuration employs two rotating shoulders, which are connected by a probe: an upper shoulder (acting on the upper surface of the parent material) and a lower shoulder (acting on the lower surface of the parent material). Due to the presence of the lower shoulder, the process loads are confined within the tool.

To date, the available literature concerning BT-FSW is still considerably less compared to standard FSW. Lally et al. [7] found that microstructures of the joints were identical for standard and BT frictions stir welded AA6056 joints but that the tensile strength and elongation were slightly lower for the BT-FSW joints than for the standard FSW joints. Wan et al. [8] reported that the weld shape of the BT-FSW joint differed from that of the weld produced using standard FSW and was similar to an hourglass shape. Liu et al. [9] investigated BT friction stir welded 6061-T6 joints and observed that the strengthening meta-stable precipitates diminished in the stir zone (SZ) and thermo-mechanically affected zone (TMAZ). However, such efforts primarily focused on Al alloys; attempts to use BT-FSW for Mg alloys are rather limited, particularly regarding the effects of the processing parameters on the microstructure and properties of the joint. Therefore, this work

* Corresponding author. Tel.: +86 29 88495226.
E-mail address: liwy@nwpu.edu.cn (W.Y. Li).
[1] He contributes most to the article.

http://dx.doi.org/10.1016/j.matdes.2014.07.023
0261-3069/© 2014 Elsevier Ltd. All rights reserved.

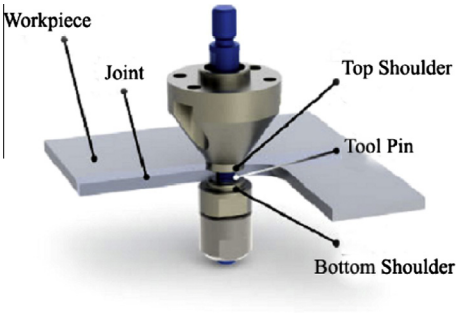

Fig. 1. Schematic of BT-FSW.

aims to investigate the effects of the tool rotational speed (ω) and welding speed (v) on the microstructure and mechanical properties of the BT friction stir welded joint in the Mg alloy AZ31.

2. Materials and methods

2.1. Materials and welding parameters

In the present study, 2 mm-thick rolled AZ31B-O Mg alloy sheets were used. The nominal chemical composition of the as-received material is presented in Table 1. The process parameters used to produce the various joints are shown in Table 2. The ratio ($\delta = \omega^2/(v \times 10^4)$: δ is dimensionless), shown in Table 2, is used in this study to discuss the effects of heat input on the microstructure and mechanical properties, because δ is the main influential factor of the resulting temperature [10]. The welding direction was perpendicular to the rolling direction.

2.2. Analysis and testing

The specimens for metallographic examination were sectioned perpendicular to the welding direction. Polished samples were obtained by employing standard metallographic procedures and were etched with a reagent consisting of 100 ml of a 2 wt% oxalate solution and 2 ml of concentrated nitric acid to reveal the micro and macrostructures. Microstructure analysis was performed using an optical microscope (OM: OLYMPUS GX51) and the Image-Pro Plus software was used to measure the grain size.

Microhardness profiles were obtained along the mid-thickness of the weld region using a Vickers hardness tester (Duramin-A300) with a load of 0.2 kg and a dwell time of 10 s. The space between indentations was 0.25 mm.

Table 1
Chemical composition (wt%) of the AZ31B Mg alloy.

Al	Zn	Mn	Si	Ni	Fe	Mg
3.01	0.9	0.5	0.04	0.005	0.005	Bal.

Table 2
Processing parameters for producing the BT-FSWed joints.

No.	ω (rpm)	v (mm/min)	δ
A	900	24	3.38
B	900	33	2.45
C	900	42	1.93
D	1050	24	4.59
E	1050	33	3.34
F	1050	42	2.63
G	1200	24	6.00
H	1200	33	4.36
I	1200	42	3.43

Tensile tests were performed on the middle parts of as-welded specimens at room temperature using a screw-driven tensile testing machine. A testing speed of 0.2 mm/min and an extensometer base length of $L_0 = 50$ mm were used. The tests were performed according to the DIN EN 10002 standard [11]. The tensile properties of each joint were evaluated using three tensile specimens cut from the same joint.

3. Results and discussion

3.1. Microstructure analysis

Fig. 2 shows the microstructure of the parent material (PM). The PM exhibits a typical rolled structure with inhomogeneous equiaxed grains [12,13]. The average grain size was determined to be 6.8 μm.

A typical macrograph of the cross-section of a BT friction stir welded sample (sample D) is shown in Fig. 3. The SZ, TMAZ and heat-affected zone (HAZ) can be clearly identified in the joint. The shape of the SZ differs from that found in BT-FSW of Al alloys. Torres [14] reported that a discernable pattern similar to "fingers" appeared in the central region of the SZ in BT-FSW 6061-T651. However, the SZ in this study is dumbbell shaped, as indicated by the dashed line in Fig. 3. Similar hourglass shapes of the SZ are observed in BT friction stir welded AA6061-T6 [9] and AA6082-T6 [8].

High magnification images of the three observed zones of Fig. 3 are presented in Fig. 4. The SZ consists of equiaxed grains, which can be attributed to the dynamic recrystallization (DRX) that resulted from the combination of frictional heating, intense plastic deformation and viscous dissipation due to the rotation of the tool during welding. Similar results have been reported in the literatures [13,15]. The grains in the upper and lower zones of all the SZs (Fig. 4b and c) are larger than those in the center zone of the SZ (Fig. 4a). The reason for the larger grains in these zones is that the temperature in the zones near the shoulders is higher. Padmanaban and Sundar [16] also found that the grains in the SZ near the shoulders were coarser than other grains in friction stir welded AZ31B joints. Fig. 4d shows the grains in the TMAZ, which are primarily equiaxed grains. It

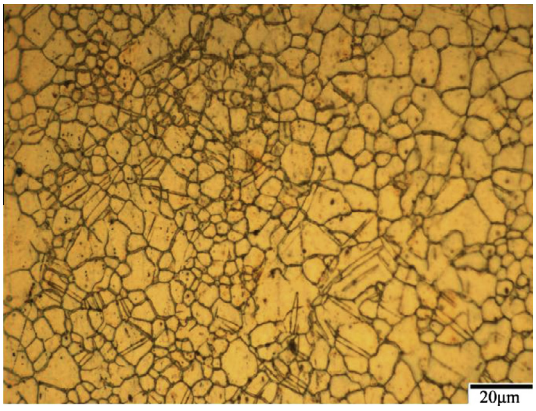

Fig. 2. Microstructure of the parent material.

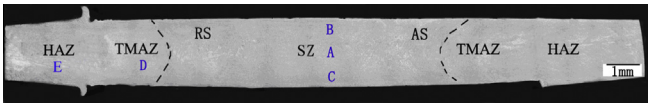

Fig. 3. A typical macroscopic image of the BT-FSWed joint.

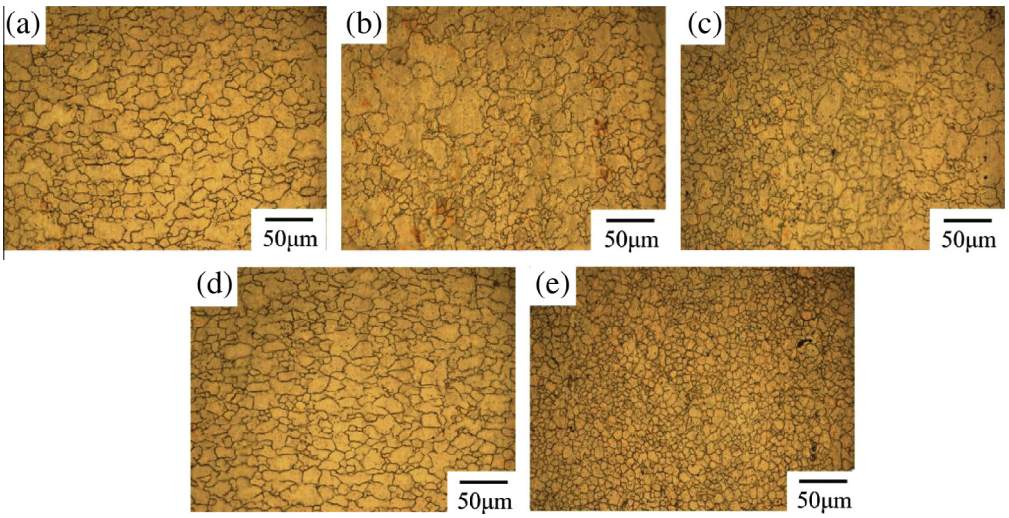

Fig. 4. Typical microscopy images of sample D: (a) central zone of the SZ, (b) upper layer of the SZ, (c) lower layer of the SZ, (d) TMAZ and (e) HAZ.

should be noted, that such a phenomenon has not previous been observed in the TMAZs of BT friction stir welded Al alloys or standard FSW of Al and Mg alloys. For BT friction stir welded Al alloys [7,8,14], the grains in the TMAZ have been reported to be severely deformed, rotated and elongated due to plastic deformation caused by interaction with the tool, and these grains generally do not recrystallize. The equiaxed grains in the TMAZ indicate that recrystallization has in fact occurred. DRX occurs more easily in Mg alloys than in Al alloys [17] because of its low stacking fault energy, few slip systems and low recrystallization temperature [18]. Thus, the TMAZ has microstructural features similar to those of the SZ, and therefore, the boundary lines between the TMAZ and SZ are not as obvious as those in Al alloy joints. However, in standard FSW of AZ61A joints investigated by Rajakumar et al. [19], elongated and deformed grains were observed in the TMAZ. These observations were explained by insufficient deformation strain and thermal exposure within this region. Compared to standard FSW, DRX during BT-FSW occurs more easily outside of the SZ due to the additional heat source represented by the second shoulder. In the HAZ (Fig. 4e), the microstructure appears similar to the PM. This result is consistent with a previous report [1].

Moreover, Fig. 5 clearly shows that the grains are smaller and more homogeneous in the TMAZ of the advancing side (AS) compared to that of the retreating side (RS). This observation is similar to the results obtained by Forcellese et al. [20] in standard friction stir welded AZ31B joints. The main reason for this result is that the strain rate in the AS is larger than that in the RS because the rotation and displacement are in the same direction in the AS. According to the reported result [21] AS also has a more extensive DRX and a faster nucleation rate.

Fig. 6 shows the microstructures in and near the flash for sample D. Coarse grains can be observed in these locations. These zones correspond to a larger shear force and higher heat input, which lead to the acceleration of grain growth.

The OM images of SZs at different δ are shown in Fig. 7. In addition, the average grain sizes of the SZs generated at different δ were measured and are plotted in Fig. 8a. It is clear that the average grain size increases with increasing δ, except for sample A (δ = 1.93).

The heat input during BT-FSW is crucial to the joint properties and is affected by welding conditions such as the rotational and welding speeds. Chang et al. [22] developed the following relations to calculate the peak temperature in the SZ:

$$\ln d = 9.0 - 0.27 \ln Z \tag{1}$$

$$T = \frac{Q}{R\left(\ln Z - \ln \frac{\omega \pi R_{SZ}}{H_{SZ}}\right)} \tag{2}$$

where d represents the grain size of the SZ, Z is the Zener–Hollomon parameter, ω is the tool rotational speed, Q is the activation energy for lattice diffusion (135 kJ/mol [23]), R is the gas constant, T is the absolute temperature in the SZ, and R_{SZ} and L_{SZ} are the average radius and depth of the SZ, respectively. R_{SZ} is assumed to equal about the radius of pin [23]. In this study, R_{SZ} and L_{SZ} are estimated to be approximately 6 mm and 2 mm, respectively.

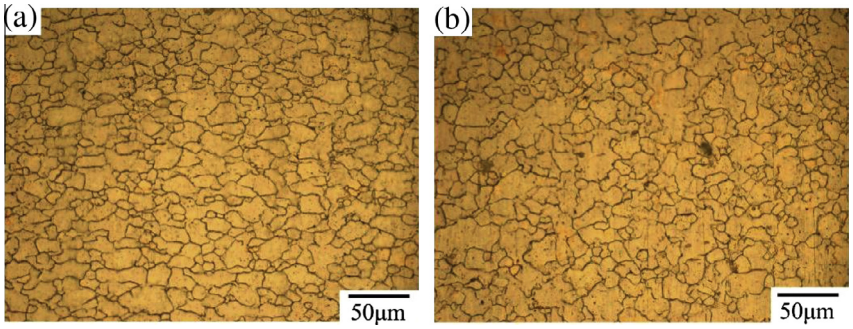

Fig. 5. Microstructure of TMAZ ((a) at advancing side and (b) at retreating side).

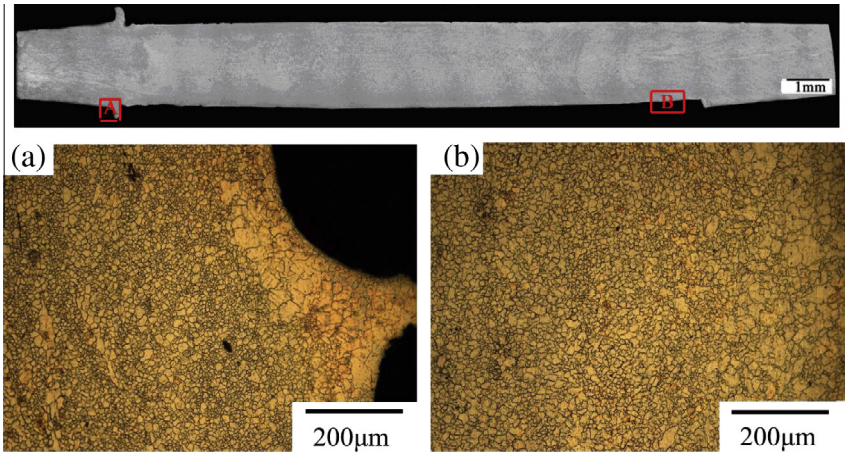

Fig. 6. Microstructures in (a) and near (b) the flash in sample D.

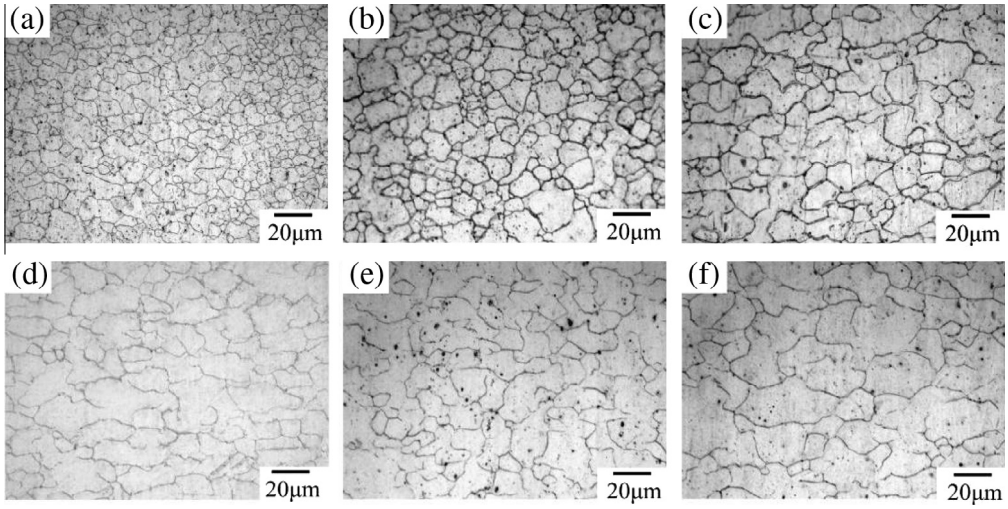

Fig. 7. Microstructures of the SZs at different values of δ: (a) 1.93, (b) 2.45, (c) 2.63, (d) 3.34, (e) 3.38 and (f) 4.59.

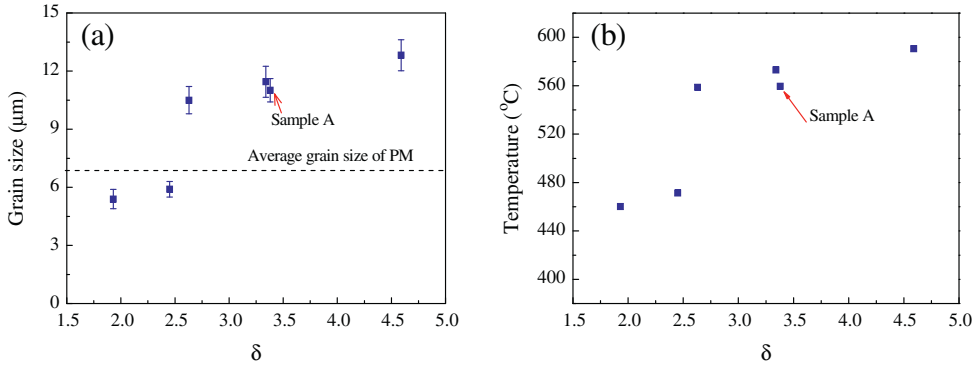

Fig. 8. Effects of δ on (a) grain size and (b) temperature in the SZ.

The SZ temperatures calculated using Eqs. (1) and (2) at different δ are plotted in Fig. 8b. It is observed that the SZ temperature could be described by the ratio δ and that it increases with increasing δ.

A larger heat input during welding provides more energy for grain growth [4]. Furthermore, higher welding speeds will lead to higher strain rates [24], which in turn activate more strain-free nucleation sites [25]. The faster the nucleation rate is, the finer the grain size will be [25]. Hence, the grain size increases as δ increases. For the AZ31B Mg alloy used in this study, the grain growth or refinement corresponds to a critical δ (i.e., 2.5). Compared to the grain size in PM, the grains in the SZ will be coarsened if $\delta > 2.5$, but on the contrary, the grains will be refined if $\delta < 2.5$.

Notably, sample B ($\delta = 2.45$) exhibits a tunnel defect in the SZ, as shown in Fig. 9. The voids are generally found close to the TMAZ in standard FSW welds [26]. There are two mechanisms for the

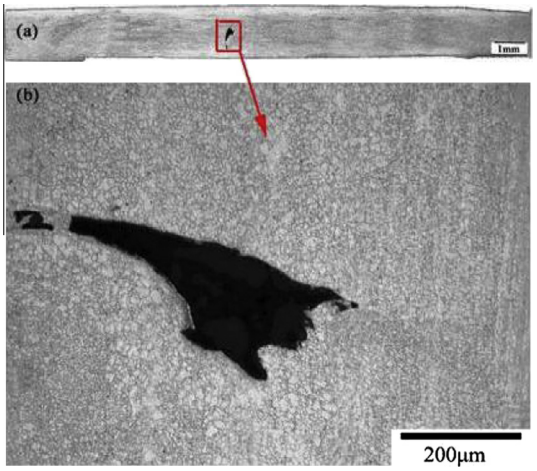

Fig. 9. Tunnel defect in the SZ of sample B.

formation of voids [12]: (i) volume deficiency and (ii) inadequate material flow and mixing. The poor stirring or mixing may be caused by low heat input; however, the voids in this work were only observed in sample B ($\delta = 2.45$), which does not correspond to the lowest heat input (Fig. 8b). Additionally, there is no obvious volume deficiency during welding. Therefore, further research may be necessary to reveal the reasons for the void formation observed in this study.

3.2. Microhardness

Fig. 10 shows the microhardness profiles along the mid-thickness of the joints welded at different δ. It is observed that the PM exhibits hardness values of 60–65 HV. Compared to the PM, a slight increase in hardness of the SZ is clearly observed at low δ (1.93 and 2.45), as shown in Fig. 10. At high δ (larger than 2.5), on the other hand, the harnesses of all joints show little variation, and the hardness values fluctuate between 50 HV and 75 HV. The above results are similar to the observations in FSWed AZ31 [23] and AZ91D [27] joints.

The changes in hardness are mainly associated with the grain size variation, dislocation density and distribution of small particles of intermetallic compounds [28–30]. The AZ31B used in this study is not a particle-strengthened material; thus, according to the Hall–Petch equation, grain refinement plays an important role in strengthening [23]. At low δ, the hardness in the SZ is larger than that in the PM due to the finer grains, which is consistent with many previously reported findings in the FSW of Mg alloys [19,28,26].

As indicated in Fig. 8a, the grain size in the SZ is larger than that in the PM when $\delta > 2.5$. Hence according to the Hall–Petch relationship, the hardness in these SZs should be smaller than that in the PM, but the hardness values in the SZ and PM are almost identical. This result may be related to other strengthening factors, such as dislocation density and residual stress [23]. Esparza et al. [28] reported that there was a slight increase in hardness in the SZs of FSWed Al or Mg alloy joints in which no reprecipitation or related aging/annealing effects occurred due to the relatively high dislocation density. In FSW AZ31 welds [31], the hardness profiles also showed slight variation and fluctuation (50–60 HV) as the rotational speed increased from 800 to 3500 rpm.

The hardness values in the AS are slightly larger than those in the RS (Fig. 10). This result can be attributed to the finer grains in the AS than in the RS. This observation agrees with the findings in FSWed AZ31 joints generated using a 'pinless' tool [20] and in FSWed Al–Mg–Sc alloy joints [32].

There are some differences in the microhardness profiles of the BT-FSWed joints in Al and Mg alloys. In BT-FSWed 6061-T651 welds, Monica [14] observed that the hardness values were inferior to those in the PM, exhibiting a "w"-shaped profile. This phenomenon has also been observed by other researchers in FSWed and BT-FSWed Al alloys [7,33]. They stated that the changing profile

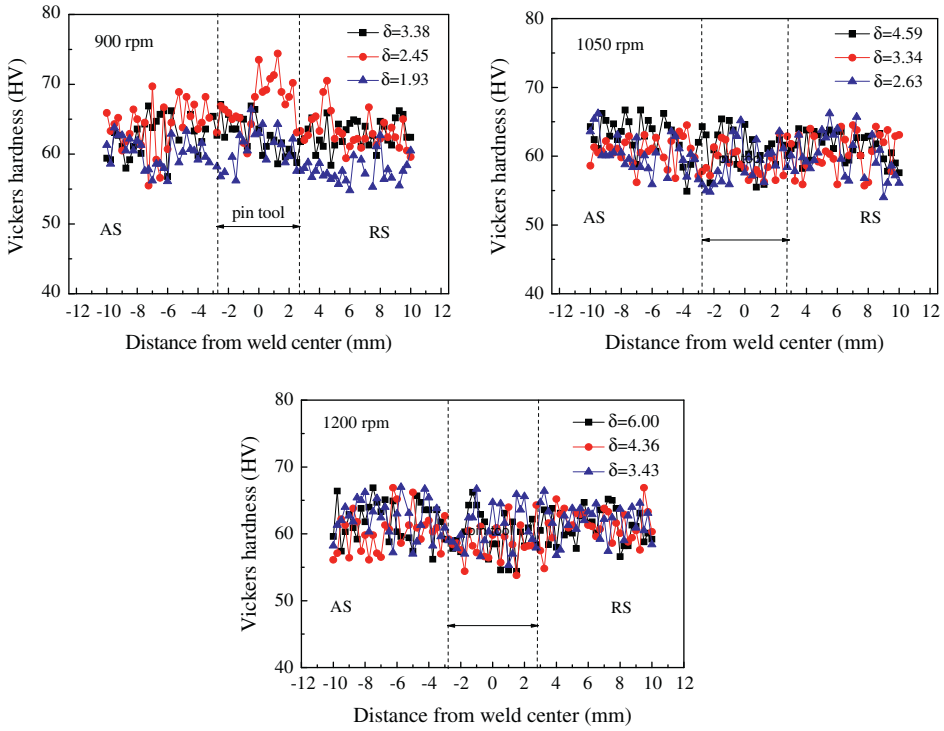

Fig. 10. Hardness profiles along the mid-thickness of joints welded under different δ.

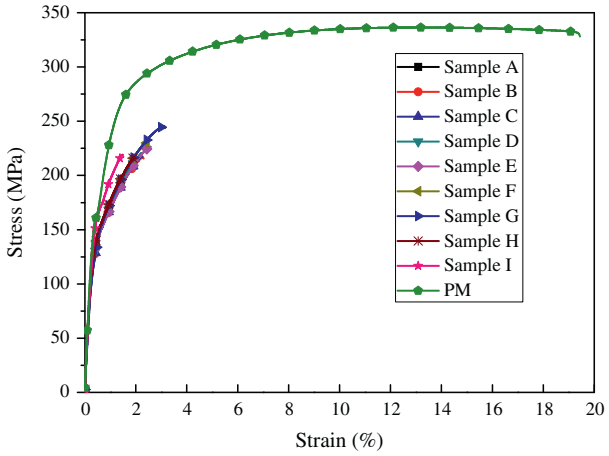

Fig. 11. Example stress–strain curves of sample A.

shape is closely associated with the distribution of the precipitation phase because the Al alloys used are precipitation-hardened alloys. In this study, however, the intermetallic phases in AZ31 are small and AZ31 is not a particle-strengthened material.

3.3. Tensile properties

To investigate the strength of the welds, tensile tests were conducted. The typical stress–strain curves of all samples and PM are presented in Fig. 11. It is clear in Fig. 11 that fracture elongations (FE) of all joints are remarkably lower than PM. A strong strain hardening on the joints has been generated which is due to the high strain rate during the BT-FSW. The strong strain hardening and microstructural gradient in welded joints cause stress concentration near the grain boundaries due to the increasing dislocations at the grain boundaries [31]. Because it is difficult to release the stress only by slip, it must rely on the twinning or crack initiation and propagation to release the stress. However, the twinning is difficult to occur, crack initiation happens and the FE of the joints becomes lower. All of the tensile test results are summarized in Fig. 12. It is clearly observed from Fig. 12 that the ultimate tensile strengths (UTS) of all joints are lower than that of the PM. In addition, the yield stresses (YS) of almost all of the joints are approximately 140 MPa, which are lower compared to the YS (165 MPa) of the PM. This result indicates that the rotational and welding speeds have only a slight impact on the YS of the joint.

With increasing welding speed, the UTS gradually increases when the rotational speed is held constant (see Fig. 12b). As shown in Fig. 8b, a higher welding speed generates lower heat, leading to a smaller grain size of the BT friction stir welded joints. Materials with a smaller grain size would impose more restrictions to dislocation movement and have a higher resistance to localized plastic deformation due to a greater number of grain boundaries [27,34]. Therefore, the UTS gradually increases at higher welding speeds when the rotational speed is held constant, which is consistent with the finding in BT-FSW 6061 joints [9].

Sample I exhibits the highest YS (156.3 MPa) and UTS (231.9 MPa) but presents a relatively small FE of ~2.04%. The FEs of all joints are remarkably lower: approximately one-eleventh of the FE of the PM. The above results demonstrate that the welding speeds remarkably impact the UTS of BT-FSWed AZ31 joints. The tensile properties of the BT friction stir welded joints in this study are lower than those of standard FSW AZ31 joints [31,35,36] because of the larger heat input imposed by the two shoulders. This phenomenon was also observed by Lally et al. [7] in standard FSW and BT friction stir welded joints in Al alloys, and they stated that the loss in UTS reaches 20% for BT friction stir welded joints in Al alloys. Yang et al. reported that the joint efficiency (a ratio of the UTS of the welded joints to the UTS of the PM) of standard FSW AZ31 joints could reach 95.2% [31], but the maximum joint efficiency is only 74% in this study.

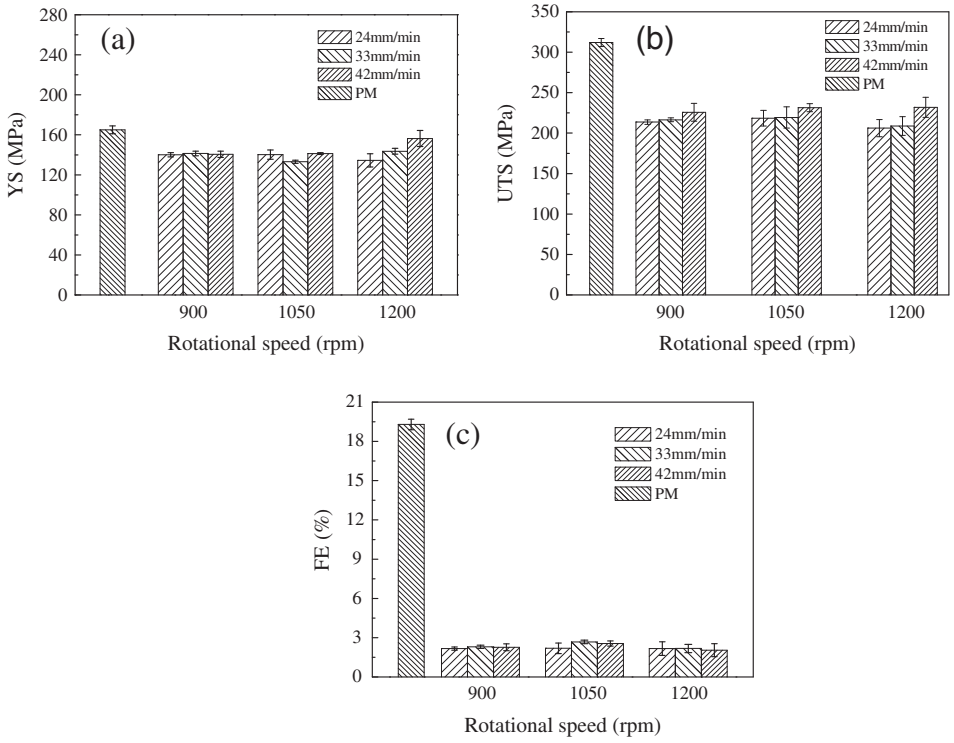

Fig. 12. Tensile test results for the PM and of all joints: (a) YS, (b) UTS and (C) FE.

4. Conclusions

The results obtained in the present study allow to draw the following conclusions:

(1) The TMAZ consists of equiaxed grains rather than the rotated and elongated grains present in the TMAZs of BT friction stir welded Al alloys and standard FSW Al and Mg alloys. The grains in the upper and lower zones of the SZ are coarser than those in the central zone of the SZ.
(2) Compared to the grain size in the PM, the grains in the SZ are coarsened if $\delta > 2.5$, but on the contrary, the grains are refined if $\delta < 2.5$. In addition, the hardness in the SZ is slightly greater than that in the PM when $\delta < 2.5$, but there are little variations in hardness throughout the joint when $\delta > 2.5$.
(3) The tensile test results demonstrate that the UTS gradually increases with increasing welding speed when the rotational speed is kept constant, but the rotational and welding speeds have only a slight impact on the YS and FE of the joint. An excellent joint with the highest YS (156.3 MPa) and UTS (231.9 MPa) is obtained, but this joint exhibits an FE as low as 2.04%.

Acknowledgements

The work reported in this study has been conducted for the reference project "Crashworthiness of Magnesium Sheet Structures" (CraMaSS). This project has been conducted within the scope of activities of the Research Platform "Lightweight Materials Assessment, Computing and Engineering Centre" (ACE). ACE is a part of the Materials Mechanics Division in the Institute of Materials Research of the Helmholtz-Zentrum Geesthacht. The authors also would like to acknowledge financial support from the Fok Ying-Tong Education Foundation for Young Teachers in the Higher Education Institutions of China (131052), the 111 Project (B08040), the Fundamental Research Funds for the Central Universities (3102014JC02010404) and the Research Fund of the State Key Laboratory of Solidification Processing (NPU, China) (108-QP-2014).

References

[1] Nagasawa T, Otsuka M, Yokota T, Ueki T. Structure and mechanical properties of friction stir weld joints of magnesium alloy AZ31. Magnesium Technol 2000;2000:383–7.
[2] Rose AR, Manisekar K, Balasubramanian V. Influences of welding speed on tensile properties of friction stir welded AZ61A magnesium alloy. J Mater Eng Perform 2012;21(2):257–65.
[3] Thomas WM, Nicholas ED, Needham JC, Church MG, Templesmith P, Dawes CJ. Friction stir welding. International Patent Application No. PCT/GB92, Great Britain Patent Application No. 9,125,978.8; 1991.
[4] Lee WB, Yeon YM, Jung SB. Joint properties of friction stir welded AZ31B-H24 magnesium alloy. Mater Sci Technol 2003;19(6):785–90.
[5] Mironov S, Motohashi Y, Kaibyshev R. Grain growth behaviors in a friction-stir-welded ZK60 magnesium alloy. Mater Trans 2007;48(6):1387–95.
[6] Zhang DT, Suzuki M, Maruyama K. Study on the texture of a friction stir welded Mg–Al–Ca alloy. Acta Metall Sin 2006;19(5):335–40.
[7] Lally AL, Alléhaux D, Marie F, Daile Oonne C, Biallas G. Microstructure and mechanical properties of the aluminium alloy 6056 welded by friction stir welding techniques. Weld World 2006;50(11–12):98–106.
[8] Wan L, Huang YX, Lv ZL, Lv SX, Feng JC. Effect of self-support friction stir welding on microstructure and microhardness of 6082-T6 aluminum alloy joint. Mater Des 2014;55:197–203.
[9] Liu HJ, Hou JC, Guo H. Effect of welding speed on microstructure and mechanical properties of self-reacting friction stir welded 6061-T6 aluminum alloy. Mater Des 2013;50:872–8.
[10] Arbegast WJ, Hartley PJ. Friction stir weld technology development at Lockheed Martin space systems-an overview. In: Fifth international conference on trends in welding research, Pine Mountain, GA, USA; 2002.
[11] DIN EN 10002. Metallic materials–tensile testing, part 1: method of test at ambient temperature. Deutsches Institut fuer Normung e.V.: materials testing standards committee; 1992.
[12] Cao X, Jahazi M. Effect of welding speed on the quality of friction stir welded butt joints of a magnesium alloy. Mater Des 2009;30(6):2033–42.
[13] Afrin N, Chen DL, Cao X, Jahazi M. Microstructure and tensile properties of friction stir welded AZ31B magnesium alloy. Mater Sci Eng A 2008;472(1):179–86.
[14] Torres M. Effect of process parameters on temperature distribution, microstructure, and mechanical properties of self-reacting friction stir welding aluminum alloy 6061-T651. El Paso: The University of Texas; 2011.
[15] Afrin N, Chen DL, Cao X, Jahazi M. Strain hardening behavior of a friction stir welded magnesium alloy. Scr Mater 2007;57(11):1004–7.
[16] Padmanaban GV, Sundar SJK. Influences of welding processes on microstructure, hardness, and tensile properties of AZ31B magnesium alloy. J Mater Eng Perform 2010;19(2):155–65.
[17] Park SHC, Sato YS, Kokawa H. Effect of micro-texture on fracture location in friction stir weld of Mg alloy AZ61 during tensile test. Scr Mater 2003;49(2):161–6.
[18] Ion SE, Humphreys FJ, White SH. Dynamic recrystallisation and the development of microstructure during the high temperature deformation of magnesium. Acta Metall 1982;30(10):1909–19.
[19] Rajakumar S, Balasubramanian V, Razalrose A. Friction stir and pulsed current gas metal arc welding of AZ61A magnesium alloy: a comparative study. Mater Des 2013;49:267–78.
[20] Forcellese A, Gabrielli F, Simoncini M. Mechanical properties and microstructure of joints in AZ31 thin sheets obtained by friction stir welding using "pin" and "pinless" tool configurations. Mater Des 2012;34:219–29.
[21] Fatmi M, Ghebouli B, Ghebouli MA, Chihi T, Abdul Hafiz M. The kinetics of precipitation in Al–2.4 wt% Cu alloy by Kissinger, Ozawa, Bosswel and Matusita methods. Physica B 2011;406(11):2277–80.
[22] Chang CI, Du XH, Huang JC. Producing nanograined microstructure in Mg–Al–Zn alloy by two-step friction stir processing. Scr Mater 2008;59(3):356–9.
[23] Commin L, Dumont M, Masse JE, Barrallier L. Friction stir welding of AZ31 magnesium alloy rolled sheets: influence of processing parameters. Acta Mater 2009;57(2):326–34.
[24] Hassan KAA, Prangnell PB, Norman AF, Price DA, Williams SW. Effect of welding parameters on nugget zone microstructure and properties in high strength aluminium alloy friction stir welds. Sci Technol Weld 2003;8(4):257–68.
[25] Pareek M, Polar A, Rumiche F, Indacochea JE. Mechanical properties and corrosion resistance of friction stir welded AZ31B-H24 magnesium alloy. In: Proceedings of the 7th international conference, Callaway Gardens resort, Pine Mountain, Georgia, USA, ASM International; 2006. p. 421.
[26] Cao X, Jahazi M. Effect of tool rotational speed and probe length on lap joint quality of a friction stir welded magnesium alloy. Mater Des 2011;32(1):1–11.
[27] Seung HC, Yutak A, Hiroyuki K. Microstructural evolution and its effect on Hall–Petch relationship in friction stir welding of thixomolded Mg alloy AZ91D. J Mater Sci 2003;38(21):4379–83.
[28] Esparza JA, Davis WC, Trillo EA, Murr LE. Friction-stir welding of magnesium alloy AZ31B. J Mater Sci Lett 2002;21(12):917–20.
[29] Razal Rose A, Manisekar K, Balasubramanian V. Effect of axial force on microstructure and tensile properties of friction stir welded AZ61A magnesium alloy. Trans Nonferrous Met Soc China 2011;21(5):974–84.
[30] Zhou L, Nakata K, Liao J, Tsumura T. Microstructural characteristics and mechanical properties of non-combustive Mg–9Al–Zn–Ca magnesium alloy friction stir welded joints. Mater Des 2012;42:505–12.
[31] Yang J, Wang D, Xiao BL, Ni DR, Ma ZY. Effects of rotation rates on microstructure, mechanical properties, and fracture behavior of friction stir-welded (FSW) AZ31 magnesium alloy. Metall Mater Trans A 2013;44(1):517–30.
[32] Subbaiah K, Geetha M, Govindaraju M, Rao SK. Mechanical properties of friction stir welded cast Al–Mg–Sc alloys. Trans Indian Inst Met 2012;65(2):155–8.
[33] Skinner M, Edwards RL. Improvements to the FSW process using the self-reacting technology. Mater Sci Forum 2003;426:2849–54.
[34] Chowdhury SH, Chen DL, Bhole SD, Cao X, Wanjara P. Friction stir welded AZ31 magnesium alloy: microstructure, texture, and tensile properties. Metall Mater Trans A 2013;44(1):323–36.
[35] Fu RD, Ji HS, Li YJ, Liu L. Effect of weld conditions on microstructures and mechanical properties of friction stir welded joints on AZ31B magnesium alloys. Sci Technol Weld 2012;17(3):174–9.
[36] Yang J, Xiao BL, Wang D, Ma ZY. Effects of heat input on tensile properties and fracture behavior of friction stir welded Mg–3Al–1Zn alloy. Mater Sci Eng A 2010;527(3):708–14.